Available online at www.sciencedirect.com
ScienceDirect
Journal of the European Ceramic Society 27 (2007) 2881–2885
www.elsevier.com/locate/jeurceramsoc

Embedded air cavity backed microstrip antenna on an LTCC substrate

M. Komulainen [a,*], J. Mähönen [a], T. Tick [a], M. Berg [b], H. Jantunen [a], M. Henry [c], C. Free [c], E. Salonen [b]

[a] *University of Oulu, Microelectronics and Materials Physics Laboratories and EMPART Research Group of Infotech Oulu, P.O. Box 4500, FIN-90014 Oulu, Finland*
[b] *University of Oulu, Telecommunication Laboratory, P.O. Box 4500, FIN-90014 Oulu, Finland*
[c] *University of Surrey, School of Electronics and Physical Sciences, Surrey GU2 7XH, UK*

Available online 28 December 2006

Abstract

One of the major challenges for next-generation, highly integrated, wireless system-on-packages (SOPs) is to integrate the antenna into the package. Due to the inherent narrow bandwidth of planar antennas on LTCC substrates that have moderate relative permittivities in the range 5–20, techniques for improving the bandwidth have to be considered in order to meet the requirements of wideband telecommunication standards. This paper presents a study of laser-micromachined air cavities embedded into an LTCC substrate, and their application in improving the bandwidth of an aperture coupled microstrip patch antenna operating at around 10 GHz. Furthermore, the effects of the air cavity on the size, gain, and radiation efficiency of the antenna are presented and discussed.

Keyword: Embedded air cavity

1. Introduction

The trend of packaging electronics into ever smaller volumes has lead to three-dimensional (3D) design approaches to highly integrated system-on-package (SOP) solutions. Multilayer, low temperature co-fired ceramic (LTCC) is one very attractive technology to increase packaging density, RF performance, and provide the functionality needed to fulfil the demands of next-generation wireless communication systems. The rapidly growing number of applications operating at microwave (3–30 GHz) and millimeter-wave (30–300 GHz) frequencies, e.g. anti-collision-radars, personal and local area networks, highlight the need for cost-efficient, reliable wireless communication modules.[1,2]

The screen printing technology associated with the standard LTCC process has traditionally been used to integrate various types of common passive components, such as resistors, capacitors, and inductors, into LTCC packages. Critical system-level microwave components such as power dividers, baluns, filters, and antennas, can also be easily integrated into this type of stucture.[3–5] The typical way to integrate an antenna is to screen print a microstrip antenna, or antenna array, onto the topmost layer of a multilayer LTCC package.[6,7]

Most commercial LTCC green tape systems have a moderate relative permittivity in the range 5–20. Since the substrate wavelength is proportional to $\varepsilon_r^{-0.5}$, the use of ceramic substrate material will reduce the antenna size when compared with implementing the antenna on PCB or air dielectrics. But it is well known that the radiation properties of microstrip antennas, such as impedance bandwidth (BW) and radiation efficiency,[8] are adversely affected as the permittivity of the substrate increases. However, the effective dielectric constant seen by an antenna could be reduced by fabricating an embedded air cavity in the substrate, beneath the radiating element. This could be a particularly useful solution for antennas operating at higher microwave and millimeter-wave frequencies, where the antenna elements will naturally have small size. For such structures, the bandwidth and radiation efficiency could be traded for antenna size, which would still retain dimensions of the order of millimeters.[9] In this way a multilayer package could still contain integrated passive components, that utilize the moderate relative permittivity of the ceramic substrate, whilst providing a

* Corresponding author. Tel.: +358 8 553 2747; fax: +358 8 553 2728.
E-mail address: mikko.komulainen@ee.oulu.fi (M. Komulainen).

0955-2219/$ – see front matter © 2006 Elsevier Ltd. All rights reserved.
doi:10.1016/j.jeurceramsoc.2006.11.012

low effective permittivity in the locality of the antenna radiating elements.

The main purpose of this paper is to introduce a microstrip antenna on an LTCC substrate that contains an embedded air cavity prepared by laser-micromachining. An air cavity-backed rectangular microstrip antenna with an aperture coupled feed for 10 GHz was designed, fabricated and measured. For comparison, the results were compared with a similar antenna without the air cavity.

2. Antenna design

Microstrip antennas screen printed on LTCC packages have several advantages. In particular, their low vertical profile, and the possibility to use an arbitrary number of dielectric layers to control the substrate thickness, make them a very attractive choice for low cost integrated antennas. Moreover, a feeding technique can be selected to facilitate easy integration of the antenna with the other microwave circuitry. The major disadvantages of microstrip antennas are narrow impedance bandwidth, poor polarization purity, and sensitivity to manufacturing tolerances.[8]

The impedance bandwidth defines a range of frequencies around the center frequency where a fixed impedance transmission line feeding an antenna is reasonably well matched to the frequency varying input impedance of the antenna. In microstrip antennas the impedance match occurs in a narrow frequency band. Typical bandwidths of a single resonator microstrip antenna with a rectangular or circular shaped radiating element are in the order of a few percent. The reflection coefficient S_{11} of a single port antenna can be calculated from the impedance of the feed line (Z_T) and the input impedance of the antenna (Z_A).

$$S_{11} = \frac{Z_A - Z_T}{Z_A + Z_T} \tag{2.1}$$

The reflection at the impedance discontinuity can also be expressed in terms of a voltage standing wave ratio (VSWR).

$$\mathrm{VSWR} = \frac{1 + |S_{11}|}{1 - |S_{11}|} \tag{2.2}$$

The total quality factor of a microstrip antenna (Q_T) is the sum of four quality factors that represent power loss mechanisms, namely dielectric losses (Q_{Diel}) due to the dielectric material, ohmic losses due to the finite conductivity of the metallization (Q_{Cond}), radiation losses with power radiated to free space (Q_{Rad}), and losses associated with surface waves (Q_{Surf}).

$$\frac{1}{Q_T} = \frac{1}{Q_{Diel}} + \frac{1}{Q_{Cond}} + \frac{1}{Q_{Rad}} + \frac{1}{Q_{Surf}} \tag{2.3}$$

The impedance bandwidth is the frequency range over which voltage standing wave ratio, VSWR, is smaller than a particular value, say S. Typically, $S = 2$, which corresponds to a return loss of 9.5 dB.

$$\mathrm{BW} = \frac{S - 1}{Q_T \sqrt{S}} \tag{2.4}$$

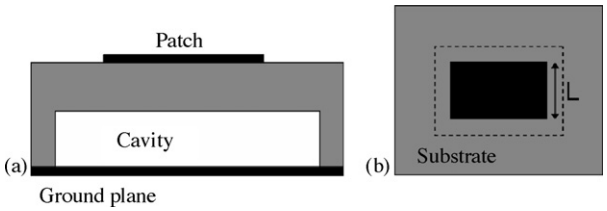

Fig. 1. (a) Side and (b) top view of a rectangular microstrip patch antenna with an embedded air cavity.

The radiation efficiency (η) of an antenna is defined as the ratio of the power radiated into free space over the input power delivered to the antenna port. It can also be expressed in terms of quality factors.

$$\eta = \frac{Q_T}{Q_{Rad}} \tag{2.5}$$

Thus, in order to improve the BW and radiation efficiency of microstrip antennas, the amount of power radiated to free space has to be increased. A possible way to reduce Q_{Rad} is to decrease the relative permittivity, or increase the height, of the substrate. Unfortunately, in multilayer LTCC packages these methods are often restricted by the moderate permittivities of the dielectric materials available, and the need for a low vertical profile to gain high packaging density. Furthermore, an increased substrate height creates the possibility of coupling significant amounts of power to unwanted surface waves.[10]

The rectangular microstrip patch antenna studied here, and which incorporates an air cavity in the substrate, is illustrated in Fig. 1 The smallest patch size is obtained with the fundamental resonant mode TM_{01}, corresponding to a patch length (L) of about half of the guided wavelength at the resonant frequency (f_r).

$$L = \frac{c}{2 f_r \sqrt{\varepsilon_{eff}}} \tag{2.6}$$

where c is the speed of light and ε_{eff} is the effective permittivity of the antenna. The effective permittivity in Eq. (2.7) is that of a mixed air-ceramic substrate (ε_{Cav}) and can be estimated from the relative permittivities of the substrate (ε_{Sub}) and air (ε_{Air}), together with the ratio of the cavity height to the full substrate thickness[9] (x_{Air}).

$$\varepsilon_{Cav} = \frac{\varepsilon_{Air}\varepsilon_{Sub}}{\varepsilon_{Air} + (\varepsilon_{Sub} - \varepsilon_{Air})x_{Air}} \tag{2.7}$$

This equation is based on a quasi-static capacitor model and it assumes that the cavity is large enough to contain all the fringing electric fields of the antenna. The effective permittivity for the antenna length calculation, given in Eq. (2.6), can be estimated from Eq. (2.7), and using formulae for transmission line models that also take into account the effects of the fringing fields at the patch edges.[10]

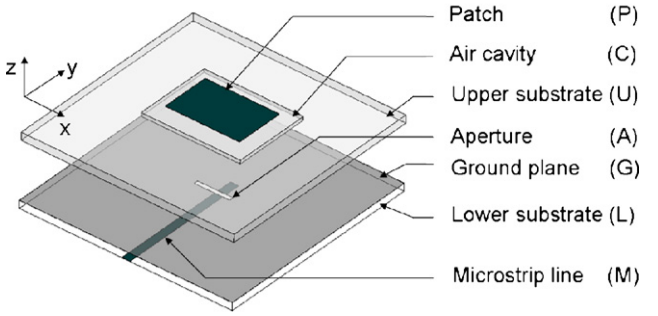

Fig. 2. Aperture coupled microstrip with an embedded air cavity. $P_x = 10.5$, $P_y = 7$, $C_x = 14$, $C_y = 11$, $A_x = 5$, $A_y = 0.6$, $L_x = L_y = U_x = U_y = G_x = G_y = 30$, $U_z = L_z = 1$, and $M_x = 1.1$, all in mm.

2.1. Aperture coupled rectangular microstrip patch antennas for 10 GHz

An aperture coupled microstrip antenna utilizes three layers of metallization and two dielectric substrates, making it feasible for implementation using multilayer technology. A microstrip transmission line on the bottom of the lower substrate is electromagnetically coupled, through an aperture in the common ground plane, to the patch on top of the upper substrate. The feed line is terminated by a quarter-wavelength open-ended stub to maximize the amount of power coupled to the antenna. Two aperture coupled microstrip patch antennas were designed to operate in the fundamental TM_{01} mode at 10 GHz. To form a uniform monolithic structure, a 1 mm ($0.03\lambda_0$) thick DuPont 951 ($\varepsilon_r = 7.8$, $\tan\delta = 0.006$ at 3 GHz) was selected as the material for both the upper and lower substrates. In the first antenna an air cavity with a height of 0.5 mm was positioned at the bottom of the upper substrate.

The antennas were analyzed using an Ansoft HFSS (version 10) electromagnetic simulator. A full-wave analysis performed with the simulator indicated a slight inaccuracy in the theoretical calculations based on Eqs. (2.6) and (2.7). The resonant length L was adjusted downwards to tune the resonant frequency to 10 GHz. The main dimensions of the designed air cavity-backed antenna are presented in Fig. 2. A second antenna without an air cavity was designed on a solid ceramic substrate, resulting in similar dimensions, but with $P_x = 6.5$, $P_y = 4.1$, $A_x = 3.5$, and $A_y = 0.4$. The simulated return losses of both antennas (Fig. 3) showed 10 dB bandwidths of 3% and 6.5%, respectively. Furthermore, the simulations indicated 6 dBi gain for the cavity antenna and 4.5 dBi for the bulk ceramic antenna, respectively.

3. Experimental procedure

The antennas were manufactured from DuPont 951 LTCC tape. The co-fired inner layer metallization was screen printed (Ami Presco) on green sheets using DP6142D silver paste. DP6160 silver paste was used for post-fired surface metallization. The printed sheets were aligned and stacked with an optical alignment system and isostatic lamination (20 MPa, 70 °C, 10 min) applied. After lamination the cavities were laser-micromachined with a Siemens Microbeam 3200 industrial

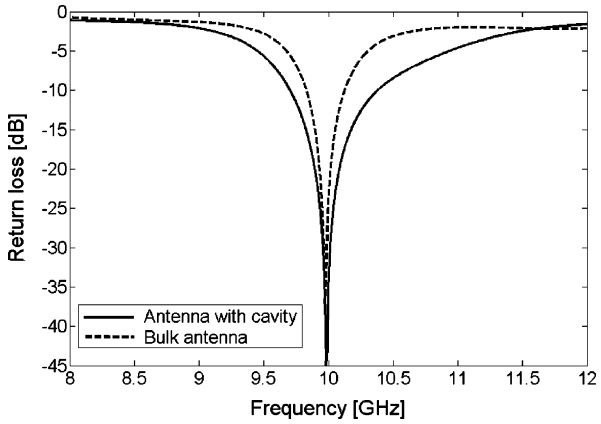

Fig. 3. Simulated return losses of aperture coupled microstrip antennas with and without an embedded air cavity.

UV laser ($\lambda = 355$ nm), followed by sintering in a box furnace (Nabertherm) at 875 °C for 20 min. An extended burnout time was used to allow efficient evaporation of all organics and to avoid blistering or cambering that is likely to happen with a large ground plane. Finally, the cavity height and substrate thickness were measured with a micrometer gauge, and the cavity surface roughness was measured with a Dektak 8 profilometer. An optical profilometer (Veeco) was used to analyze the test structure's surface roughness and cavity height when optimizing the laser-micromachining parameters.

4. Results and discussion

The final cavity antenna was an assembly of two fired monolithic substrates glued together. Altogether, the antenna was formed of 10 layers of DP951AX tape, and the final thickness of the assembly was 2060 μm. A cross-section of the antenna is shown in Fig. 4. The reference antenna without an air cavity was prepared using the same materials and processes, but in this case the structure was monolithic, and comprised only one multilayer substrate. Laser-micromachining was chosen for the air cavity preparation since it enabled cavity depths to be formed independently of the tape thickness. The cavity was laser-machined after lamination, thus avoiding the complicated processing steps normally faced when laminating a green body with cavities.[11,12]

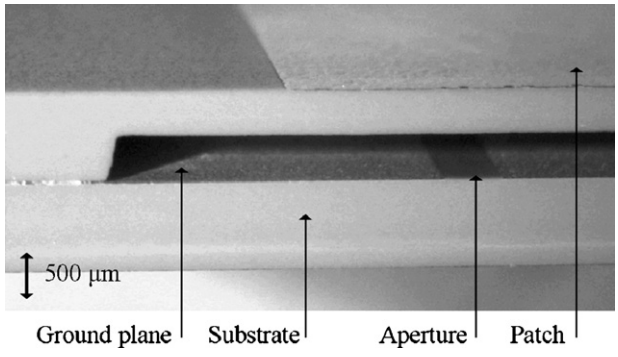

Fig. 4. A cross-section image of the antenna showing the laser-micromachined cavity.

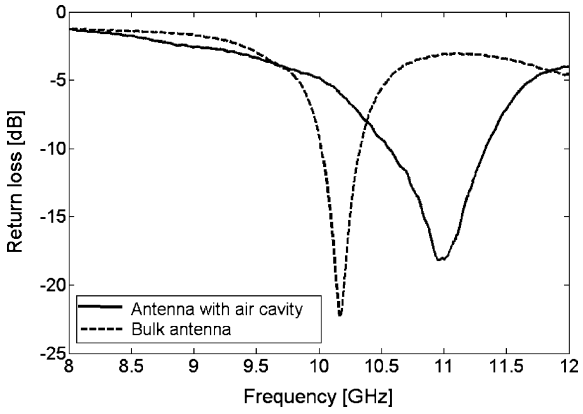

Fig. 5. Measured return losses of aperture coupled microstrip antennas with and without an embedded air cavity.

The laser-micromachining parameters were optimized by varying the pulse repetition rate between 20 kHz and 80 kHz, the power between 0.4 W and 3.2 W, and the beam scanning speed between 50 mm/s and 200 mm/s. Increasing the scan speed and decreasing the pulse repetition rate and power resulted in better surface roughness, but it also reduced the depth reached with a single sweep of the cavity area. Choosing the appropriate laser-machining parameters is thus a compromise between surface quality and processing time.

The *Z*-direction sintering shrinkage of the LTCC tape in this design was measured to be 16.7%. To achieve the designed fired cavity depth of 500 μm, a 600 μm deep cavity had to be micromachined into the laminate. Alternating the beam sweep directions was observed to improve the surface quality, and the laser-machining parameters were optimized to give a single-sweep depth that would result in the desired cavity when repeated. The parameters chosen for the pulse repetition rate, power, and scan speed were 20 kHz, 3.2 W, and 150 mm/s, respectively. The hatching of the cavity area was done in 10 μm increments, which was best suited for the 15 μm beam diameter used. These process parameters produced a cavity with a depth of 100 μm with a single sweep. The direction of the sweep was altered 90° between each sweep. A 600 μm deep cavity processed in the aforementioned way had a surface roughness of 1.5 μm and a fired cavity depth of 500 μm.

The measured return loss of the cavity antenna (Fig. 5) showed a 10% upward frequency shift. The shift was probably caused by the somewhat cambered cavity roof on the electrically measured samples. The measured BWs of the cavity and non-cavity antenna were 6.8% and 3.2%, respectively. Moreover, the far field measurements showed maximum gains at the center frequency of 5.4 dBi for the cavity antenna and 3.2 dBi for the bulk ceramic antenna. The measured radiation patterns for the both antennas are presented in Figs. 6 and 7.

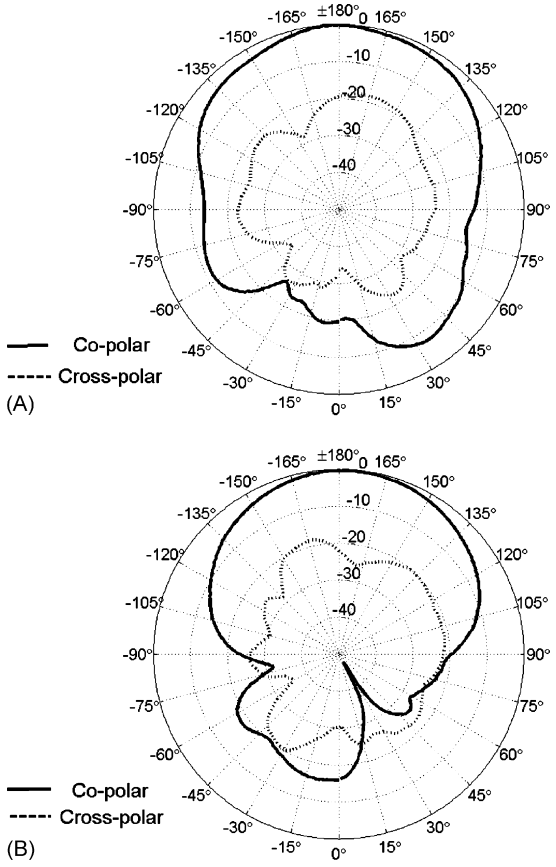

Fig. 6. (A) Measured *E*-plane (*YZ*-plane) and (B) *H*-plane (*XZ*-plane) radiation patterns for antenna with embedded air cavity.

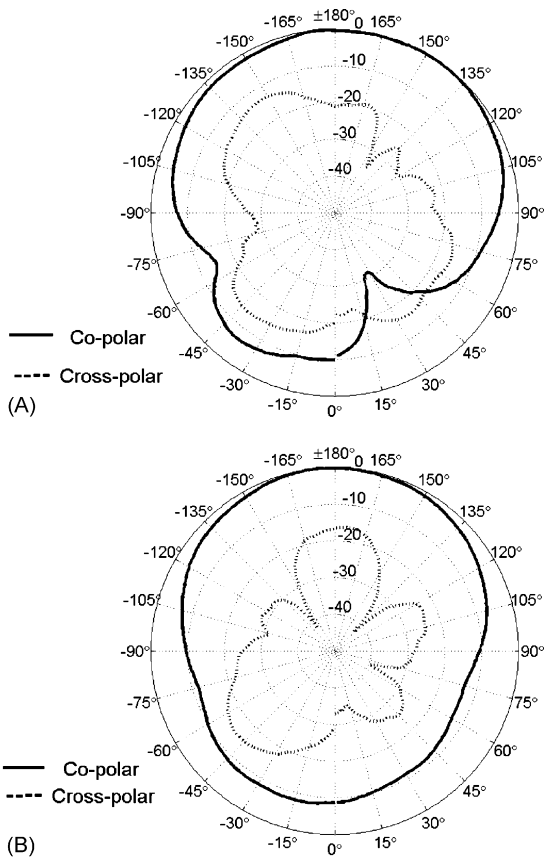

Fig. 7. (A) Measured *E*-plane (*YZ*-plane) and (B) *H*-plane (*XZ*-plane) radiation patterns for bulk ceramic antenna.

The results proved that the BW of an aperture coupled microstrip antenna was approximately doubled by fabricating an embedded air cavity into the substrate, while still maintaining a reasonable antenna size of 7 mm × 10.5 mm for system-on-package assemblies. The method of fabricating the embedded air cavity for the antenna structures offers a flexible way to produce complex cavity shapes and cavity depths that are independent of tape thickness, while still providing quick turnaround time between designs. As shown, fairly predictable performance of the air cavity antenna was also achieved. The results also suggest that in the second preparation cycle special attention should be paid to avoiding deformation of the cavity roof. In the future, the laser-aided micromachining method that has been discussed could also be used to produce air cavity structures to form true monolithic packages for microwave applications.

5. Conclusion

This paper has proposed a microwave microstrip antenna on an LTCC substrate applicable to low cost integrated SOP packages. A laser-machined embedded air cavity was used to enhance the impedance bandwidth by reducing the effective permittivity of the substrate around the antenna. Furthermore, a laser-micromachining method of fabricating the embedded air cavities was proposed along with detailed machining parameters.

Acknowledgements

The authors (M.K., J.M., T.T.) acknowledge the Jenny and Antti Wihuri foundation, the Finnish Society of Electrical Engineers, the Foundation of Technology, the Seppo Säynäjäkangas Foundation, the Emil Aaltonen Foundation, the Ulla Tuominen Foundation, and the Tauno Tönning Foundation for financial support of the work. Finnish Funding Agency of Technology and Innovation (project number 52292) and its industrial partners are also acknowledged.

References

1. Lee, J.-H., De Jean, G., Sarkar, S., Pinel, S., Lim, K., Papapolymerou, J. *et al.*, Highly integrated millimeter-wave passive components using 3-D LTCC system-on-package (SOP) technology. *IEEE Trans. Microwave Theory Tech.*, 2005, **53**, 2220–2229.
2. Jantunen, H., Kangasvieri, T., Vähäkangas, J. and Leppävuori, S., Design aspects of microwave components with LTCC technique. *J. Eur. Cer. Soc.*, 2003, **23**, 2541–2548.
3. Kangasvieri, T., Hautajärvi, I., Jantunen, H. and Vähäkangas, J., Miniaturized low-loss Wilkinson power divider for RF front-end module applications. *Microwave Opt. Technol. Lett.*, 2006, **48**, 660–663.
4. Lee, B. H., Park, D. S., Park, S. S. and Park, M. C., Design of new three-line balun and its implementation using multilayer configuration. *IEEE Trans. Microwave Theory Tech.*, 2006, **54**, 1405–1414.
5. Lee, J.-H., Pinel, S., Papapolymerou, J., Laskar, J. and Tentzeris, M. M., Low-loss LTCC cavity filters using system-on-package technology at 60 GHz. *IEEE Trans. Microwave Theory Tech.*, 2005, **53**, 3817–3824.
6. Li, R., DeJean, G., Maeng, M., Lim, K., Pinel, S., Tentzeris, M. M. *et al.*, Design of compact stacked-patch antennas in LTCC multilayer packaging modules for wireless applications. *IEEE Trans. Adv. Pack.*, 2004, **27**, 581–589.
7. Seki, T., Honma, N., Nishikawa, K. and Tsunekawa, K. A., 60-GHz multilayer parasitic microstrip array antenna on LTCC substrate for system-on-package. *IEEE Microwave Wireless Comp. Lett.*, 2005, **15**, 339–341.
8. Pozar, D. M., Microstrip antennas. *Proc. IEEE*, 1992, **80**, 79–91.
9. Papapolymerou, I., Franklin Drayton, R. and Katehi, L. P. B., Micromachined patch antennas. *IEEE Trans. Ant. Prop.*, 1998, **46**, 275–283.
10. Garg, G., Bhartia, B., Bahl, I. and Ittipiboon, A., *Microstrip Antenna Design Handbook*. Artech House, Norwood, Mass, 2001, p. 845.
11. Vaed, K., Akbar, S. A., Madou, M. J., Lannutti, J. J. and Cahill, S. S., An additive micromolding approach for the development of micromachined ceramic substrates for RF application. *IEEE J. Microelectromech. Syst.*, 2004, **13**, 514–525.
12. Panther, A., Petosa, A., Stubbs, M. G. and Kautio, K. A., Wideband array of stacked patch antennas using embedded air cavities in LTCC. *IEEE Microwave Wireless Comp. Lett.*, 2005, **15**, 916–918.